

Detailed Experimental Survey of the Transonic Flow Field in a Rotating Annular Turbine Cascade

P.-A. Gieß, F. Kost
 DLR, Institut für Strömungsmechanik, Göttingen, Germany

Abstract

An annular cascade of turbine profiles was tested in the wind tunnel for rotating cascades at DLR, Göttingen. In this facility investigations of the relative flow through a rotor cascade were done while the absolute inlet flow is purely axial and the relative inlet flow is determined by the circumferential speed of the rotor corresponding to the velocity triangles. Detailed experimental research concerning the 3-D flow field was carried out using an L2F-velocimeter and pneumatic probes; the flow field under investigation was determined by the isentropic downstream Mach number at midspan ($Ma_{2is} = 1.1$).

First, at midspan local flow quantities (mean velocity, angle, Reynolds shear stress, turbulence intensity) were obtained using laser velocimetry. Additionally the static pressure on the blade surface was determined at 48 positions. The homogeneous flow quantities (velocity, flow angle, losses) were taken at four axial positions - one upstream and three downstream of the cascade. By comparing these results with linear cascade data, the influence of rotational effects on the 2-D flow field can be detected.

Second, the radial variation of the flow was investigated at several axial positions (upstream, within and downstream of the cascade) using the above mentioned experimental methods. Additionally the boundary layers on hub and tip were measured by means of a "fish mouth type" pitot probe. These results give an impression of the 3-D flow field, which is dominated by the blade geometry and rotational effects.

All these experimental data can serve to validate computer codes because of the detailed measurement programme as well as the reproducible and completely documented "experimental boundary conditions".

Nomenclature

h	relative blade height $\frac{(r-r_{hub})}{(r_{tip}-r_{hub})}$
L_{Bi}, L_{Ax}	true chord length, axial chord length
Ma	Mach number

t	pitch
p	pressure
R	gas constant
T	temperature
Tu_u, Tu_v	streamwise, transverse turbulence
w, u	relative, absolute velocity
x, y, z	cartesian coordinates
x, ϕ, r	cylinder coordinates
y_{BL}	distance from hub, tip
β	relative flow angle
β_s	stagger angle
δ	boundary layer thickness
κ	ratio of specific heats
μ	axial velocity density ratio
ρ	density
subscripts:	
0	total flow condition
1,2	homogeneous flow upstream, downstream
is	isentropic
Kon	on the blade surface
v, w	absolute, relative frame of reference
BL	boundary layer

Introduction

Manufacturers spend much effort on the improvement of turbomachines operating in jet engines as well as in power stations. The primary energy used should remain constant or even decrease when increasing the efficiency by increasing the process temperature and pressure. In addition the increasing efficiency can contribute to reducing the number of stages and therefore saving weight and costs. To succeed here, a deeper understanding of the aerodynamic details in the flow field and improved numerical simulations of the major phenomena is necessary. Within the national research programme "AG-TURBO" detailed experimental and numerical investigations were performed to contribute to this task. The experiments considering 2-D flow in linear cascades as well as 3-D flow in annular cascades were performed to give data which can serve to validate improved 2-D and 3-D Navier-Stokes computer

L_{bi}	=	30.439 mm	r_{hub}	=	238.0 mm
t/L_{Bi}	=	0.755	r_{tip}	=	274.0 mm
β_S	=	66.2°			
β_1	=	140.0°			

Table 1: Cascade geometry at midspan; radii of the test section

codes. For this purpose the midspan blade contours of a gas turbine stage were used to form a stator and a rotor cascade. Cylindrical blades were used to build up both the linear 2-D cascade as well as the annular 3-D cascade.

Most of the papers considering either 3-D experimental investigations or 3-D numerical studies focus on special details of the flow field, see [1, 2, 3, 4]. The present contribution gives an overview of the transonic flow through a rotating annular turbine cascade. The results were collected applying conventional measurement techniques (with probes and pressure tappings) and non intrusive techniques (L2F-velocimetry). The complete experimental data were documented in [9, 10] where further details of the experimental setup and of the evaluation procedure are given.

Profile and cascade geometry

The blade contour and the cascade geometry were taken from the midspan section of a gas turbine rotor stage. According to this contour cylindrical blades were eroded to this shape with an accuracy of approximately 0.07% at the leading edge and the trailing edge and of approximately 0.02% elsewhere. For the coordinates see [8] and for the cascade geometry see tab. 1. 70 blades were mounted on the test wheel forming an annular cascade with the above given geometry at midspan. Because of the radial blade spacing some geometric variables depend on the radius, as for example the pitch, the throat ($\approx \pm 7\%$), and the inlet flow angle ($\approx \pm 2^\circ$).

Wind tunnel

The experiments were performed in the wind tunnel for rotating cascades at DLR, Göttingen. A detailed discussion of its operation range and of its design goals are given in [5]. This facility was built to investigate the relative flow through annular cascades for turbines as well as for compressors within a wide range of parameters, as Reynolds number, Mach number, inlet flow angle, flow turning etc. The inlet flow is purely axial due to the absence of any swirl generator. This set-up avoids disturbing the homogeneous flow field by the wakes of the guide vanes or by radial equilibrium effects in helical flow fields. It also gives

some advantages when measuring and evaluating the flow data, especially in the case of total temperature.

The wind tunnel operates in closed cycle mode while a four stage radial compressor drives dried air. The air passes the heat exchanger to extract the thermal energy added by the compressor, the settling chamber with grids and honey combs to straighten the flow, enters the annular test section after a strong contraction, and finally reaches the compressor again via a pipe system. The correct inlet flow direction with respect to the rotating relative frame of reference had to be determined by the corresponding circumferential velocity of the test wheel, because of the absence of any guide vanes. A vacuum pump or a compressor serves to vary the total pressure within $20\text{kPa} \leq p_{01} \leq 130\text{kPa}$ allowing for independent variation of Mach number and Reynolds number. The total temperature is kept constant at about 300°K .

The ratio of the test section diameters at hub and tip ($r_{hub}/r_{tip} = 0.869$) was chosen in order to obtain 2-D flow at least at midspan. This was not achieved totally as shown later; nevertheless the flow field at midspan can still be compared to those obtained in a 2-D cascade. Differences of the results are due to 3-D effects as radial equilibrium or radial blade spacing. Tip clearance is avoided by means of an abradable material mounted into a slot of the casing. This allows the blades to touch the casing without damaging the test wheel; the resulting steps of approximately 0.1mm - 0.2mm at the cascade inlet plane and exit plane can be neglected.

For the measurements the flow parameters have to be adjusted within the absolute frame of reference corresponding to the flow parameters in the relative frame of reference. For constant flow conditions (some hours during the L2F-measurements) the compressor and the heat exchanger have to operate within an appropriate regime; therefore the total pressure was chosen to be $p_{01} = 50\text{kPa}$.

Measurement technique and data reduction

Probe measurements

Wake traverses were done using fixed probes within the absolute frame of reference. Because of the rotation of the cascade (blade passing frequency approximately 5kHz) the local flow values at the position of the probe are highly unsteady. The probes used detect only time averaged values total pressure, total temperature, and flow direction, that means the homogeneous flow quantities in case of the probe being located far enough downstream. To compute the flow quantities within the relative frame of reference in general five flow values have to be measured within the

absolute frame of reference. Upstream of the cascade some simplifications can be applied because of the axial flow direction and the easy measurement of total temperature and total pressure. Applying Euler’s turbine equation and/or the continuity equation some flow quantities downstream depend on measured flow values upstream, thus less than five values are sufficient to determine the flow field. Summarizing descriptions of these possibilities for evaluating the probe measurements are given in [6, 7] and in detail in [9].

The presented measurements were evaluated using Euler’s turbine equation to avoid the measurement of the total temperature downstream. Therefore upstream of the cascade total temperature, T_{0v1} , total pressure, p_{0v1} , and static pressure, p_1 , are measured, while $\alpha_1 = 0.0^\circ$, due to the axial flow condition. Downstream of the cascade the total pressure, p_{0v2} , the flow direction, α_2 , and the static pressure, p_2 , have to be measured. With the rotational speed of the annular cascade these values are sufficient to describe the homogeneous flow field. Note, because of the special set-up used here the total temperature as well as the total and the static pressure upstream do not depend on the radius. As there is axial flow up to the rotating cascade and as the total temperature is constant everywhere in the inlet the total temperature in the relative system yields $T_{0w2} = T_{0v1} + \frac{\kappa-1}{2\kappa R} \omega^2 r^2$. Only assuming that in the relative system no work is done by the fluid.

Boundary layer measurements upstream of the cascade at hub and tip were done using a “fish mouth type” pitot probe. In order to get velocity profiles, boundary layer thickness, form factors, etc. the evaluation of the total pressure profiles was done within the absolute frame of reference. Assuming that inside the boundary layer the static pressure is constant and agrees with p_1 , the flow is adiabatic, and finally total pressure and total temperature agree with the values taken in the settling chamber. The boundary layer edge is defined as the point where the velocity reaches 99% of the upstream velocity.

Pressure distribution on the blade surface

The static pressure distribution on the blade surface is detected using 16 absolute pressure transducers, which were mounted on the test wheel near the axis. Each transducer serves for reading three different pressure tapings by means of a switching mechanism. A slip ring device transfers the electrical signals of the transducers from the rotating frame of reference to the absolute one. Just under the blade surface - from hub to tip - a radial hole was eroded which is connected to the switching mechanism. The pressure distribution for one constant radius was taken af-

ter drilling the tapings into this pipe; for measurements at another radius this tapings had to be closed and the new ones had to be drilled. Doing this successively from tip to hub the pressure distribution was taken at different radii (90%, 75%, 50%, 25%, 10% blade height). The necessary pressure correction because of centrifugal forces, the calibration of the transducers, and some other details of the pressure measurement are described in [6].

L2F-Measurements

To investigate the flow field especially within the rotating blade passages a Laser-Two-Focus velocimeter (L2F) was used, as described in detail in [7, 11]. The measurements of the velocity components were done in axial and circumferential direction, while neglecting the radial component due to the assumption of cylindrical stream surfaces. The used L2F-system generates two highly focussed light beams in the probe volume which act as a ‘light gate’ for tiny particles in the flow. The scattered light provides two successive pulses with a time delay proportional to the velocity component perpendicular to the direction of the two foci and to their separation. The foci had a diameter of $8\mu\text{m}$ and were separated by $207\mu\text{m}$. As seeding of the flow in order to increase the data rate oil droplets of $0.3\mu\text{m}$ diameter were used. They were produced using a special seeding generator and were injected into the flow in the settling chamber.

The mean flow angle is provided by turning the second laser beam around the first one and thus accumulating velocity distributions at a certain number of angles. The whole measurement procedure was PC-controlled, automatically changing the L2F-angle, measuring the velocity distributions at the specified angles, and storing the data for each angle. The measurement position in the rotor pitch is delivered by an angular encoder. A statistical evaluation procedure gives the desired mean flow values (u, v) and the mean fluctuation values. Normalizing the mean fluctuation values with the local flow velocity, u , the turbulence level and the Reynolds shear stresses were obtained.

From the velocity the corresponding Mach number $Ma_w = u / \sqrt{\kappa R T_{0w2} - \frac{\kappa-1}{\kappa} w^2}$ was derived using the total temperature from the above formula.

The flow field at midspan Characteristic structures of the flow field

Flow visualisation using the Schlieren technique is not possible at the wind tunnel for rotating cascades. On the other hand, due to the fact that the ratio of diameters at hub and tip is close to unity, the midspan flow should behave like a 2-D flow. There-



Figure 1: Schlieren photo of the 2-D flow field ($Ma_{2is} = 1.1$)

for a good agreement of flow characteristics can be seen by comparing the Schlieren photo (fig. 1) taken in the Göttingen wind tunnel for linear cascades to the Mach number distribution (fig. 2) at midspan which was determined with the L2F-system. In detail, there is a trailing edge shock causing boundary layer separation on the suction side just upstream of the cascade exit plane. The pressure side shock travelling towards the suction side of the adjacent blade can be detected as well as the reflected shock system indicating a laminar separation bubble at $x_{Ax}/L_{Ax} \approx 0.8$. Both shocks pass the wake of the blades at $x_{Ax}/L_{Ax} \approx 1.15$ to 1.25 and $x_{Ax}/L_{Ax} \approx 1.35$. Near the leading edge the flow expands strongly on the suction side as well as on the pressure side giving no evidence of any separation.

Doing the L2F-measurements 32 points per pitch were taken, enough to indicate the dominant structures of the flow field as the trailing edge shock travelling downstream and the wakes of the blades. The pressure side shock running to the adjacent blade is hard to see. For more details as the shock boundary layer interaction on the suction side or the trailing edge separation a higher spatial resolution is necessary.

The flow field upstream of the cascade

Details of the upstream flow field are shown in fig. 3. Far upstream ($x_{Ax}/L_{Ax} = -0.947$) the flow direction meets exactly the design value of $\beta_1 = 140^\circ$, without any circumferential variation. The constant

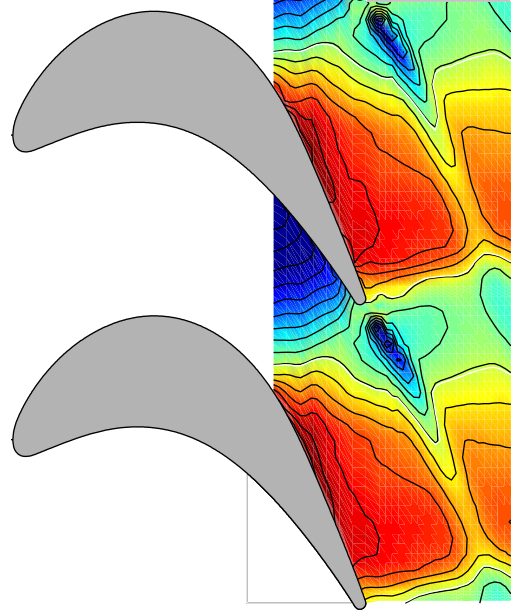


Figure 2: Mach number distribution at midspan from L2F-velocimetry ($Ma_{2is} = 1.1$); the white line indicates sonic velocity

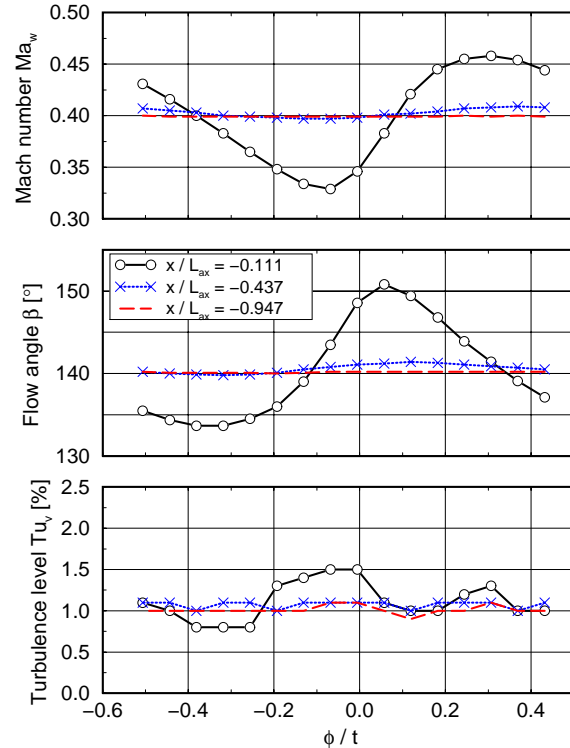


Figure 3: Inlet flow at midspan (Mach number, flow angle, and turbulence level from L2F-velocimetry)

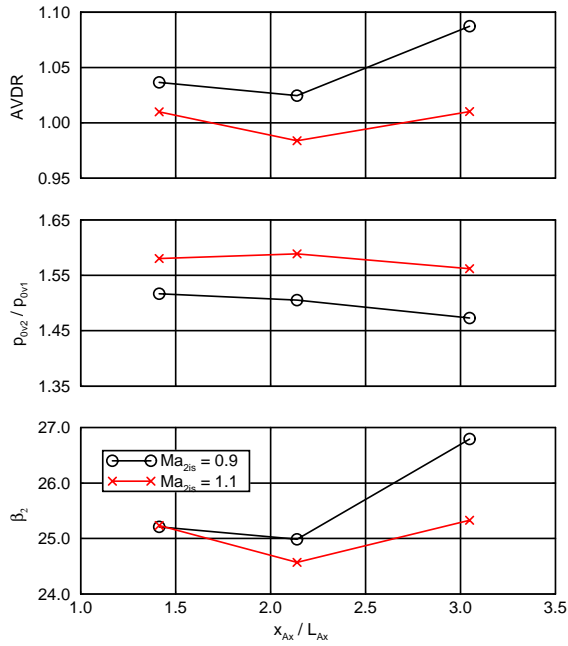


Figure 4: Downstream flow at midspan (flow angle, total pressure loss, axial velocity density ratio from probe measurements)

Mach number of $Ma_1 = 0.400$ fits very well the theoretical value of $Ma_{1th} = 0.392$ assuming choked 2-D conditions. The slight difference of these values should be due to the boundary layer displacement on hub and tip. This homogeneous flow field is influenced by the blade row when approaching the cascade inlet plane. A slight circumferential variation of flow direction and Mach number appears first at $x_{Ax}/L_{Ax} = -0.437$. The displacement of the fluid due to the blades gives a strong circumferential dependency of the flow direction ($134^\circ \leq \beta_1 \leq 151^\circ$) and the Mach number ($0.33 \leq Ma_1 \leq 0.46$) in the plane at $x_{Ax}/L_{Ax} = -0.111$. The turbulence level, Tu_v , of the upstream flow is constant at about 1% and begins to increase in the plane closest to the cascade.

The flow field downstream of the cascade

To detect the homogeneous flow quantities downstream of the annular cascade probe measurements were done in planes located at $x_{Ax}/L_{Ax} = 1.410$, 2.140 and 3.049. The flow angle, β_2 , the pressure ratio, p_{0v2}/p_{0v1} , and the axial velocity density ratio, $\mu = (\rho_2 w_2 \sin \beta_2) / (\rho_1 w_1 \sin \beta_1)$, are shown in fig. 4. Comparing the total pressure ratio there are only minor differences within the first and the second plane while there is a decrease of about 2% to the third plane. The flow angle is $\beta_2 \approx 25.0^\circ$ within the first two planes and remains constant in case of $Ma_{2is} = 1.1$ while increasing of about 2.0° in case of $Ma_{2is} = 0.9$ when

approaching the third plane. This dependency of β_2 causes the variation of μ within the three measurement planes. The deviation of the μ -value from unity especially in the subsonic case gives first hints towards the fact that the assumption of cylindrical stream surfaces is not correct. The distortion of the stream surfaces even at midspan is caused by the increasing boundary layers at hub and tip, the mixing of the fluid, and the secondary flow vortices which are generated within the blade passages and which increase while they travel downstream.

Radial variation of the flow field

The upstream boundary layer

Upstream of the cascade different boundary layers develop at hub and tip. At the hub the boundary layer starts at the stagnation point of the interior contour of the test section. The velocity of the incoming fluid is relatively small and increases rapidly because of the strong contraction of the cross section. Only just upstream of the blade row there are constant flow conditions. At the tip the boundary layer starts far upstream in the settling chamber when the fluid passes the honey combs and grids. In the settling chamber and upstream of the center body there are extended regimes of constant flow velocity. Additionally there are two points where small separation bubbles may occur. All this contributes to the development of a boundary layer of finite thickness which then decreases due to the strong acceleration of the fluid up to the regime of constant flow conditions. Constant flow conditions are indicated one axial chord length upstream by giving the same pressure on the walls and outside the boundary layer (fig. 5). Constant flow conditions are detected by the L2F-measurements at midspan, too (fig. 3). The boundary layer edges are at about 1mm from the hub and 2.5mm from the tip. Normalising the velocity profiles with the values at the boundary layer edge (fig. 5) on hub and tip the same development can be seen. It fits very well the potential law $(y/\delta = (u/u(\delta))^n)$ for turbulent boundary layers without pressure gradient using $n = 8$, as the dashed line indicates. When entering the boundary layer the turbulence level increases due to the velocity fluctuations, see fig. 6. 10% from the hub - outside the boundary layer - there is the same turbulence level as at midspan, while 10% from the tip - near the boundary layer edge - the turbulence level increases significantly. This indicates a much thicker boundary layer at the tip than on the hub.

The flow field downstream of the cascade

Near hub and tip the homogeneous flow values vary within a wide range, while there are only slight

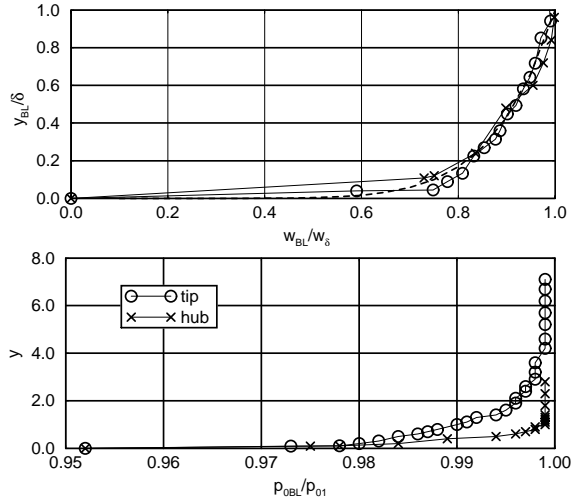


Figure 5: Total pressure and normalised velocity profiles in the boundary layer from probe measurements at $x_{Ax}/L_{Ax} = -0.947$ (upstream)

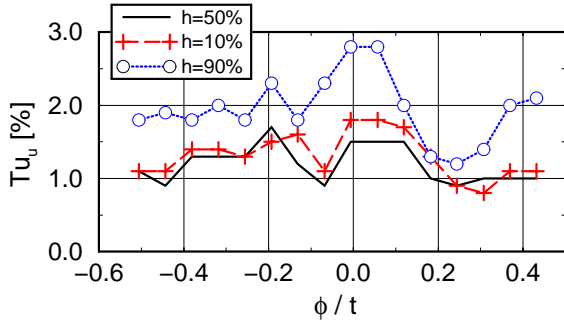


Figure 6: Turbulence level measurements using a L2F-velocimeter at $x_{Ax}/L_{Ax} = -0.111$ (upstream)

differences near midspan (fig. 7). From $h = 0.2$ to 0.6 there are nearly constant flow conditions in both planes. Due to the radial equilibrium the Mach number decreases from 1.15 to 1.05 , while the flow angle varies within $\pm 0.5^\circ$ around the average value of $\beta_2 = 25.5^\circ$, and the pressure loss remains constant at about 5% . Note, that there is a radial component of the flow velocity, which could not be taken into account with the probes used. Furthermore there are no cylindrical stream surfaces with constant thickness because of the developing secondary flows near the hub and tip. Third, the radial interpolation of the static pressure from hub to tip gives only approximate values because of the radial distortion of the iso-Mach lines especially near the hub (fig. 8).

Because of the special experimental set-up there is a higher absolute velocity of the fluid than within the real stage. This results in overestimated pressure losses near the walls of hub and tip. Nevertheless the most important mechanisms of the flow through the

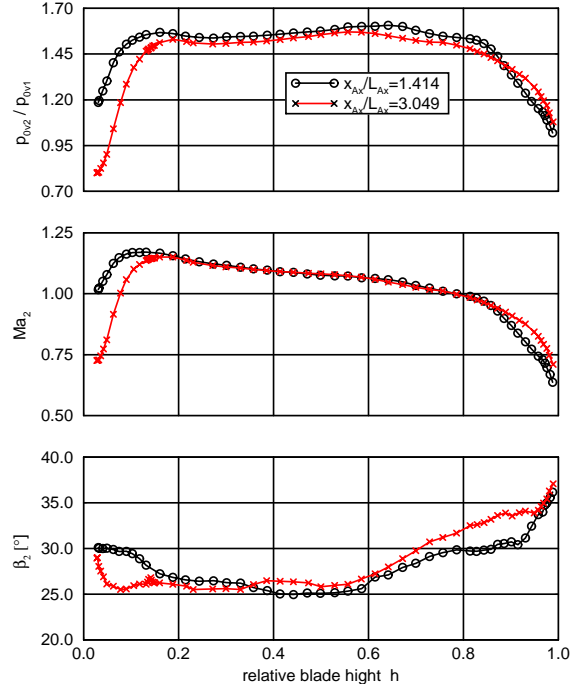


Figure 7: Mach number, total pressure loss, flow angle (wake traverses, $Ma_{2is} = 1.1$)

cascade are described correctly.

Approaching the hub in the plane $x_{Ax}/L_{Ax} = 1.410$ the Mach number increases up to 1.2 at $h \approx 0.1$ before decreasing to 1.0 close to the wall. The total pressure remains constant up to $h \approx 0.1$ and decreases rapidly to $p_{0v2}/p_{0v1} \approx 1.20$ near the wall, while the flow angle increases up to 30.0° . This development of these flow quantities only fits together, if there is a strong secondary flow near the wall generated by the deflection of the fluid within the blade row. These vortices were detected by the laser measurements (fig. 8). The local Mach number and the flow direction are shown in the same plane $x_{Ax}/L_{Ax} = 1.410$ where the probe measurements were done. The iso-lines indicate the marked counter rotating vortices near the hub. Proceeding downstream to the plane $x_{Ax}/L_{Ax} = 3.049$ the probe measurements give an idea about the development of the secondary flow with a dramatic decrease of the pressure to $p_{0v2}/p_{0v1} \approx 0.75$ and a decrease of the Mach number down to $Ma_2 \approx 0.75$. That means close to the wall ($h \leq 0.1$) there is an entirely subsonic flow field.

Approaching the tip the development of the homogeneous flow values indicate an extended secondary flow region ($h \geq 0.6$). Within the upper 20% of the cross section there is a completely subsonic flow field where the total pressure rapidly decreases.

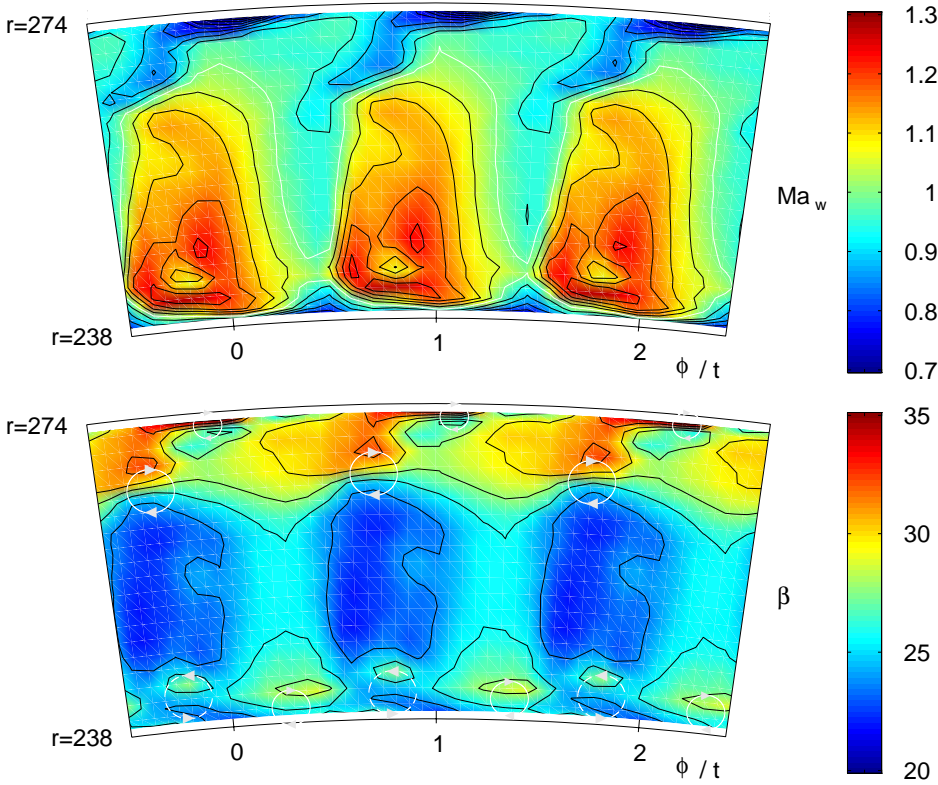


Figure 8: Mach number, flow angle from L2F-measurements ($Ma_{2is} = 1.1$, $x_{Ax}/L_{Ax} = 1.41$)

From the laser measurements vortices can be detected at $h \approx 0.8$ and $\phi/t \approx -0.2 + n$ and $h \approx 0.95$ and $\phi/t \approx n$ ($n = 0, 1, 2, \dots$).

The flow field within the cascade

The pressure distribution on the blade surface (fig. 9) was measured in 5 radial sections. Up to approximately 60% of the axial chord the blade loading increases from hub to tip while decreasing in the rear part.

On the pressure side there seems to be a separation bubble for $h = 0.1$ at 10% axial chord. The constant Mach numbers on the blade surface cause a growth of the boundary layer which decreases rapidly when the strong acceleration - up to sonic velocity at the throat - acts on the fluid.

On the suction side the pressure distribution indicates that there are laminar separation bubbles for $h = 0.10$ and 0.25 at about 80% to 90% axial chord. The constant Mach number (corresponding to the base pressure approximately) on the last 10% of the blade for $h = 0.75$ and 0.90 indicate a very thick boundary layer that may be separated. A shock boundary layer interaction forming a laminar separation bubble can not be deduced from the pressure distribution at

midspan.

Conclusion

Detailed measurements using conventional techniques (probes, pressure tappings) and non intrusive ones (L2F-velocimetry) give beneficial information about the three dimensional flow field of an annular rotor cascade.

There are strong secondary flow fields up to 20% blade height at the hub and down to 60% from the tip.

The secondary flow vortices near hub and tip were detected by L2F-velocimetry.

Even with short blades the assumption of cylindrical stream surfaces of constant thickness is not applicable any more.

The L2F-measurements indicated a strong distortion of the stream surfaces, especially near hub and tip.

Acknowledgement

The reported investigations were supported by the german ministry of education, science, research and technology under project no. 032 6800 F within the framework of the national AG-TURBO programme. The authors gratefully acknowledge this support.

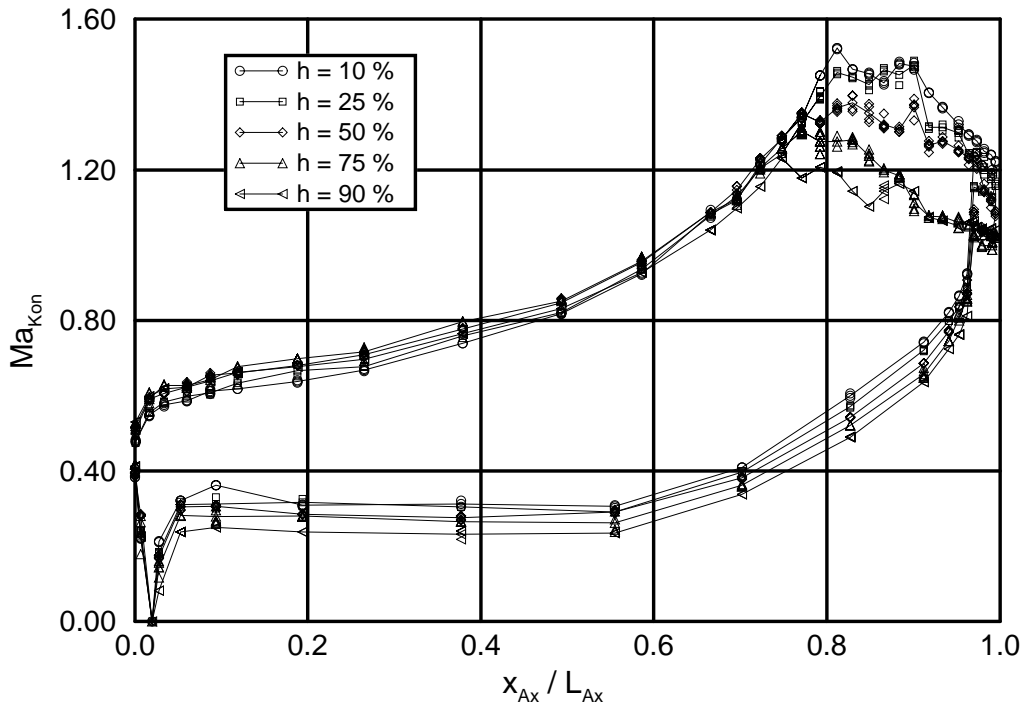


Figure 9: Mach number distribution on the blade surface ($Ma_{2is} = 1.1$)

References

- [1] Hodson, H. P. and J. S. Addison; *Wake-Boundary Layer Interactions in an Axial Flow Turbine Rotor at Off-Design Conditions*; ASME, technical paper 88-GT-233 (1988)
- [2] Heider, R., J.M. Duboue, B. Petot, G. Billonnet, V. Couaillier and N. Liamis; *Three-Dimensional Analysis of Turbine Rotor Flow Including Tip Clearance*; ASME, technical paper 93-GT-111 (1993)
- [3] Yamamoto, A., J. Tominaga, T. Matsunuma and E. Outa; *Detailed Measurements of the Three-Dimensional Flows and Losses Inside an Axial Flow Turbine Rotor*; ASME, technical paper 94-GT-348 (1994)
- [4] Tisserant, D. and F. Breugelmans; *Rotor Blade-to-Blade Measurements Using Particle Image Velocimetry*; ASME, technical paper 95-GT-99 (1995)
- [5] Amecke, J. and F. Kost; *3.2 Rotating Annular Cascades*; in Hirsch, Ch. (Ed.); *Advanced Methods for Cascade Testing*, AGARD AG 328, 1993
- [6] Bräunling, W.; *Untersuchungen zum Einfluß der Konizität auf die Kennwerte rotierender Turbinen-Ringgitter im transsonischen Geschwindigkeitsbereich*; VDI-Forschungsheft Nr. 627, VDI-Verlag, Düsseldorf, 1985
- [7] Kost, F.; *Längswirbelentstehung in einem Turbinenlaufrad mit konischen Seitenwänden*; DLR-FB 93-13, DLR, Köln, 1993
- [8] Gieß, P.-A.; *Nachlauf- und Druckverteilungsmessungen bei transsonischer und inkompressibler Durchströmung ebener Turbinengitter zur Verifikation von Navier-Stokes-Verfahren*; IB 223 - 94 A 07, DLR, Göttingen, 1995
- [9] Gieß, P.-A.; *Nachlauf-, Druckverteilungs- und Grenzschichtmessungen in der transsonischen Strömung durch ein rotierendes Ringgitter mit zylindrischer Gasturbinenlaufradbeschaufelung*; IB 223 - 96 A 10, DLR, Göttingen, 1996
- [10] Kost, F.; *Messung des transsonischen Geschwindigkeitsfeldes mit dem L2F-Velocimeter in einem rotierenden Ringgitter mit zylindrischer Gasturbinenlaufradbeschaufelung*; IB 223 - 96 A 11, DLR, Göttingen, 1996
- [11] Schodl, R.; *A Laser-Two-Focus (L2F) Velocimeter for Automatic Flow Vector Measurements in Rotating Components of Turbomachines*; J. Fluid Eng., vol. 102, pp. 412-419 (1980)